Energy 238 (2022) 121948

Contents lists available at ScienceDirect

Energy

journal homepage: www.elsevier.com/locate/energy

Optimal planning of intra-city public charging stations

Haiyang Lin [a, b], Caiyun Bian [c], Yu Wang [a], Hailong Li [d, e, f, *], Qie Sun [a, e, **], Fredrik Wallin [d]

[a] Institute of Thermal Science and Technology, Shandong University, Jinan, 250061, China
[b] John A. Paulson School of Engineering and Applied Sciences, Harvard University, Cambridge, MA, 02138, USA
[c] School of Economics, Nankai University, Tianjin, 300071, China
[d] School of Business, Society and Engineering, Mälardalen University, Västerås, 72123, Sweden
[e] Institute for Advanced Technology, Shandong University, Jinan, 250061, China
[f] School of Mechanical Engineering, Hubei University of Arts and Science, Xiangyang City, Hubei Province, 441053, China

ARTICLE INFO

Article history:
Received 19 March 2021
Received in revised form
27 August 2021
Accepted 28 August 2021
Available online 1 September 2021

Keywords:
Electric vehicle (EV)
Public charging stations
Geographic information system (GIS)
Agent-based model
Optimal planning

ABSTRACT

Intra-city Public Charging Stations (PCSs) play a crucial role in promoting the mass deployment of Electric Vehicles (EVs). To motivate the investment on PCSs, this work proposes a novel framework to find the optimal location and size of PCSs, which can maximize the benefit of the investment. The impacts of charging behaviors and urban land uses on the income of PCSs are taken into account. An agent-based trip chain model is used to represent the travel and charging patterns of EV owners. A cell-based geographic partition method based on Geographic Information System is employed to reflect the influence of land use on the dynamic and stochastic nature of EV charging behaviors. Based on the distributed charging demand, the optimal location and size of PCSs are determined by mixed-integer linear programming. Västerås, a Swedish city, is used as a case study to demonstrate the model's effectiveness. It is found that the charging demand served by a PCS is critical to its profitability, which is greatly affected by the charging behavior of drivers, the location and the service range of PCS. Moreover, charging price is another significant factor impacting profitability, and consequently the competitiveness of slow and fast PCSs.

1. Introduction

In recent years, the electrification of the transportation sector is thriving. Electric Vehicles (EVs) have shown clear advantages, such as environmental friendlyness, flexible operation, energy storage etc. However, it must be noted that the transfer from internal combustion engine vehicles to EVs should be accompanied by a highly renewable energy mix in order to maximize the benefit. For the fossil fuel dominated power production, indirect pollution still exists [1]. In countries with high penetration of renewable energy, different measures, such as tax reduction, subsidies, and extra local benefits, e.g., free parking, have been implemented to motivate the transition from petroleum-fueled vehicles to EVs [2]. Although EVs' penetration is rapidly increasing, reaching 7.2 million units in 2020 globally, EVs account for only a tiny market share [3,7].

Range anxiety is one of the most concerning issues for EV users and potential owners [5], and intra-city Public Charging Stations (PCSs) play a critical role in relieving range anxiety [6]. Recent years have seen a rapid development of public EV charging infrastructure. In 2019, the installed Publicly Accessible Chargers (PACs) reached 0.8 million in the world and accounted for an increasing share in the total installed light-duty vehicle chargers [7]. However, the number of installed PACs is far below the global EV stock. The underdevelopment of PCSs is regarded as the most significant barrier to EV penetration [8]. It is, therefore, essential to boost the intra-city PCSs installation and motivate the associated investment.

Many efforts have been focused on optimizing the location and size of intra-city PCSs. For example, Cavadas et al. [9] and Sun et al. [10] conducted location optimization of PCSs based on residents' travel behaviors to maximize satisfied charging demand with constraints of a fixed budget. Xi et al. [11] and Wang et al. [12] employed the utility theory to maximize PACs' utilization with budget constraints. Zhu et al. [13] formulated a minimization problem for attaining minimal cost, including construction costs of PCSs and EVs' travel fuel costs. A method that can search for the

* Corresponding author. School of Business, Society and Engineering, Mälardalen University, Västerås, 72123, Sweden.
** Corresponding author. Institute of Thermal Science and Technology, Shandong University, Jinan, 250061, China.
E-mail addresses: hailong.li@mdh.se (H. Li), qie@sdu.edu.cn (Q. Sun).

https://doi.org/10.1016/j.energy.2021.121948

Nomenclature

Acronyms

ABTCM	Agent-based trip chain model
CA	Commercial area
EV	Electrical vehicle
EVSE	Electric vehicle supply equipment
FCLM	Flow-capturing location model
FPCS	Fast public charging station
GIS	Geographic information system
MA	Mixed-use area
MILP	Mixed integer linear programming
NA	Natural area
O-D	Origin-destination
O&M	Operation and maintenance
OPC	Off-peak charging
PAC	Publicly accessible chargers
PCS	Public charging station
RAA	Residential apartment area
ROI	Return on investment
RVA	Residential villa area
SCLM	Set-coverage location model
SOC	State of charge
SPCS	Slow public charging station
TMP	Traffic measurement point
UC	Uncontrolled charging
WA	Working area

Parameters and variables

i	Index of potential locations for intra-city PCSs, with a total number of I
j	Index of cells and corresponding demand nodes, with a total number of J
k	Index of TMPs in a cell, with a total number of K
m	Index of trips
t	Index of hours, with a total number of T during the simulation
lu	Index of land use types, $lu \in \{R, W, P\}$, with R, W, P representing residential, working and public land use type, respectively
z	Index of existing PCSs
Pr	Profit of newly-built PCSs
p	Charging price per minute
x	Binary indicator for whether to build a PCS
q	Hourly charging demand covered by PCS
n	Number of EVSE in a PCS
pw	Charging power of EVSE in a PCS
c	Total cost of a PCS
c^{rent}	Land rental costs
c^{inv}	System investment costs
$c^{O\&M}$	Operation and maintenance costs
c^{ele}	Electricity costs
c^{park}	Parking fee
c^{EVSE}	Investment costs of an EVSE
LT	Life span of an EVSE
D	Potential charging demand
Dl	Charging demand at a demand node
rp	Binary variable for the coverage ability of a newly-built PCS
lp	Euclidean distance between a demand node and a newly-built PCS
L	Service range of the PCS
y	Maximum number of EVSE that can be installed at a PCS
N	Maximum number of PCSs to be deployed
p_d	Departure place
T_d	Departure time
d_t	Driving distance
t_d	Driving time
p_e	Destination place
t_p	Parking time
SOC_0	Original SOC
E	Electricity consumption per kilometer
C	Capacity of and EV battery
Da	Hourly average charging demand
f	Amount of traffic flow
A	Area covered by a type of land use
Dc_j	A vector containing hourly charging demand at the node of cell j
De	Charging demand on a demand node covered by an existing PCS
re	Binary variable denoting the coverage ability of an existing PCS
le	Euclidean distance between a demand node and an existing PCS
P	Total output power of an existing PCS

shortest paths and a multiple domination model were adopted in studies [14,15] to minimize the number of PCSs while satisfying all the charging demand. In addition, the costs of electrification and energy transmission loss were also taken into account in PCS planning to reduce the impacts on grid reliability in Refs. [16,17]. Integration of solar power [18] and wind power [19] integration becomes a new principles for PCS development to realize a low carbon future. However, most of the previous studies focused on serviceability rather than the profitability of PCSs. It is also noted that high investment and low utilization of PCSs might lead to a low chance of profiting [20]. How intra-city PCSs should be deployed to gain maximal profits is vital for stakeholders and has not been comprehensively studied. There is a clear knowledge gap about quantitatively evaluating the economic performances of intra-city PCSs.

To quantitatively assess the economy of intra-city PCSs, it is important to consider the key factors affecting the profit of PCSs, including location, charging demand, charging price, and the types of Electric Vehicle Supply Equipment (EVSE) in the PCS [8]. Planning intra-city PCSs is different from planning inter-city PCSs. Inter-city PCSs are usually constructed in highway networks to serve 'on-route charging', and fast charging is the priority [21,22]. Intra-city PCSs mainly meet 'end-route charging' demands for short-distance trips. Intra-city charging often happens at parking locations, varying with time of the day and type of land use [23,24]. Therefore, planning of intra-city PCSs needs to consider the spatial and temporal distribution of charging demand.

Modeling techniques of EV charging demand in the formulation of PCS planning problem have obtained extensive academic attentions. In the existing literature, the most popular methods are Flow-Capturing Location Models (FCLMs) and set-coverage location models (SCLMs). FCLM, which was firstly introduced by Hodgson [25], uses Origin-Destination (O-D) flows to express the refueling/charging demand and aims to enable drivers to complete O-D trips

with multiple stations on the transport network. Adopting a traffic equilibrium model, He et al. [26] considered driving range limitations, and Chen et al. [27] investigated the impacts of drivers' time sensitivities on charging patterns. In contrast to the fixed and static shortest path principle, Yang [28] relaxed the assumptions on route choice and allowed small deviation from shortest path to simulate diverse user behaviors, and Li et al. [29] developed a multi-period optimization model to simulate the dynamics in the charging network. In other studies, FCLMs were extended to capture the stochastic nature of EV charging demand [21,30]. However, the applications of FCLMs are usually limited to the planning of refueling stations and inter-city PCSs that satisfies long distance travel demands, while SCLMs show better accuracy in intra-city PCS planning [31]. SCLM, proposed by Toregas [32], aggregates short distance charging demand in parking lots, which are generated using the method of node-based geographical segmentation. The disadvantage of SCLM is that charging demand is usually estimated based on the population density and vehicle ownership density, while ignores the dynamic and stochastic nature of EV travel and charging behaviors [33]. There have been a few studies that refined SCLMs to explicitly assess the mobility of EVs. Vazifeha et al. [34] conducted individual EV trajectory analysis based on call detail records. Bai et al. [35] formulated a data-driven optimization problem based on the GPS trajectory data of thousands of vehicles. It is noted that the charging patterns of EVs were usually over-simplified in the literature.

For intra-city PCS planning, public charging demand should be distinguished from private ones. This is usually handled by assuming simplified travel and charging patterns that EVs are only charge at home or public areas [36,37]. However, in reality, EVs tend to be charged both at home and in public areas [38]. Some studies transformed the demand partition problem into choice criterion problems and associated demand levels with types of land use [39,40]. Luo et al. [41] investigated the temporal and spatial distribution of EV charging demand by acquiring EV parking distribution at different types of land uses. However, in these studies, the charging patterns of EVs and urban land uses are usually over-simplified, which can lead to significant deviations from real charging demand profiles.

Through reviewing the related works, the following gaps have been identified: (i) there is a lack of analysis about the economy of intra-city PCSs, which is crucial for motivating investment; (ii) there has not been a computationally effective method that can model both temporal and spatial distributions of charging demand and localize the demand corresponding to real-world urban areas; and (iii) there has not been a categorization method that can distinguish public charging demand from private charging demand.

To fill these gaps, this paper proposes a novel method that can consider the impacts of charging behaviors and urban land uses on optimizing the location and size of PCS in order to maximize the profits. An Agent-Based Trip Chain Model (ABTCM) is adopted to generate dynamic and stochastic charging demand; and a cell-based geographic partition method is conducted to localize the generated public charging demand to real-world urban areas. To optimize the siting and sizing of intra-city PCSs, a GIS-based Mixed Integer Linear Programming (MILP) optimization model is formulated. The proposed method is applied to Västerås, a Swedish city, to evaluate the impacts of service range, economic parameters and charging strategies on the profit of intra-city PCSs.

Following this introductory section, the remainder of the paper is structured as follows: In Section 2, the methodology for optimizing the planning of intra-city PCSs is presented. Section 3 applies the proposed methods to Västerås, Sweden, as a case study. Section 4 reports and discusses the results and Section 5 concludes the paper with a summary of key findings.

2. Methodology

The structure of the proposed method is depicted in Fig. 1. Charging revenues and costs, land rental costs and system investment costs are taken into consideration to assess the economic benefits of intra-city PCSs.

The charging demand generated from the Agent-Based Trip Chain Model (ABTCM) is localized to each geographic cell according to the type of land use and the volume of traffic flow. Then, the economic benefits of newly built PCSs are maximized with the MILP model considering charging revenues and costs, land rental costs and system investment costs. Charging revenues and costs are calculated based on electricity price, charging price of the selected EVSE and charging demand covered by the PCS. Land rental costs are determined by the locations of intra-city PCSs, which are selected from the potential intra-city parking locations identified by the GIS model. Investment costs are decided by the type and number of EVSE, which are dependent on the land use type and the magnitude of charging demand. The details of each sub model are introduced in the following sections.

2.1. The Mixed Integer Linear Programming model

2.1.1. The objective function

The siting and sizing of all PCSs are optimized simultaneously in maximizing the total profit of newly-built intra-city PCSs. The objective function is:

$$Max\ Pr\left(x_i, n_i, q_{i,t}\right) = \sum_{i=1}^{I}\left[p_i{*}x_i{*}\sum_{t=1}^{T} q_{i,t} \Big/ \left(n_i * pw_i\right) - c_i\right] \tag{1}$$

$$x_i = \begin{cases} 1 & \textit{if PCS } i \textit{ is planned to be built} \\ 0 & \textit{otherwise} \end{cases} \tag{2}$$

where Pr is the profit of newly-built PCSs in the study area; p is the charging price per minute; x is a binary variable representing whether a PCS is built at a certain location, which is determined by Eqn (2); q represents the hourly charging demand covered by the PCS; n and pw denote the number and charging power of EVSE at the PCS, respectively; c is the total cost of a PCS; I represents the total number of potential locations; T represents the total number of hours during the simulation; and subscripts i and t denote the index of potential locations for intra-city PCSs and the index of the hour of the day.

The total cost of a PCS consists of land rental cost (c^{rent}), system investment cost, (c^{inv}), fixed Operation and Maintenance (O&M) cost, ($c^{O\&M}$), and electricity cost (c^{ele}), which are calculated as Eqns (3)–(7). The fixed O&M costs are assumed to be 3% of the investment costs [42].

$$c_i = c_i^{rent} + c_i^{inv} + c_i^{O\&M} + c_i^{ele} \tag{3}$$

$$c_i^{rent} = c_i^{park}{*}n_i \tag{4}$$

$$c_i^{inv} = c_i^{EVSE}{*}n_i \tag{5}$$

$$c_i^{O\&M} = 3\%{*}LT{*}c_i^{inv} \tag{6}$$

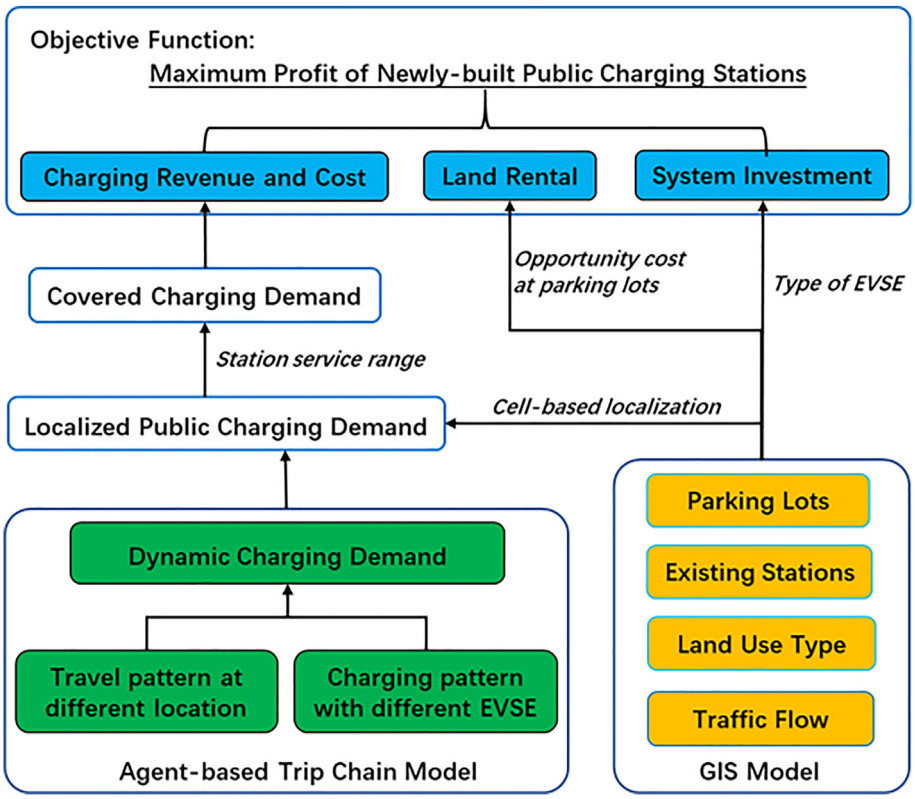

Fig. 1. Overview of the modeling framework.

$$c_i^{ele} = c_{ele} * \sum_{t=1}^{T} q_{i,t} \tag{7}$$

where c^{park} represents the parking fee for parking and installing charger during the period of use; and c^{EVSE} and LT stand for the investment costs of an EVSE and its life span, respectively.

2.1.2. The constraints

1) Constraints on charging demand

The hourly charging power covered by the ith PCS, $q_{i,t}$, is constrained by the potential charging demand nearby ($D_{i,t}$) and the total installed charging capacity (n_i*pw_i), as shown in Eqns (8–10). The potential charging demand at a PCS ($D_{i,t}$) is gathered from surrounding nodes according to Eqn (11), the demand nodes have to be in the PCS's service range (Eqn (12)) and cannot be assigned to another PCS (Eqn (13)).

$$q_{i,t} \le D_{i,t} \tag{8}$$

$$q_{i,t} \le n_i * pw_i \tag{9}$$

$$q_{i,t} \ge 0 \tag{10}$$

$$D_{i,t} = x_i \sum_{j=1}^{J} \left(Dl_{j,t} \cdot rp_{i,j} \right) \tag{11}$$

$$rp_{i,j} = \begin{cases} 1 & lp_{i,j} \le L \\ 0 & lp_{i,j} > L \end{cases} \tag{12}$$

$$\sum_{i=1}^{I} x_i \cdot rp_{i,j} \le 1 \tag{13}$$

where D denotes the potential charging demand that originates within the service range of a PCS and could be possibly covered by the PCS; j is the index of cells and corresponding demand nodes; J represents the total number of cells and corresponding demand nodes, which are further explained in Section 2.3; Dl is the charging demand at a demand node; rp is a binary variable denoting the coverage ability of a newly-built PCS; lp represents the Euclidean distance between a demand node and the PCS; and L represents the service range of the PCS.

2) The limits of the number of EVSE

Eqns (14) and (15) respectively define the upper bound and lower bound of the number of EVSE.

$$n_i \ge x_i \tag{14}$$

$$n_i \le y_i \cdot x_i \tag{15}$$

where y_i represents the maximum number of EVSE that can be installed at a PCS.

3) The limit of the total number of PCS

Eqn (16) describes the maximum number of PCS that will be

deployed.

$$\sum_{i=1}^{I} x_i <= N \tag{16}$$

where N is the maximum number of PCSs that can be deployed in the study area.

2.2. Dynamic EV charging demands at different land use types

To simulate the potential charging demand in urban areas, an ABTCM model is used, which can capture the dynamics of EV trips at three different land use types, corresponding to seven trip purposes (Fig. 2).

The trips of an EV agent in the ABTCM are characterized by six types of parameters: the place and time of departure, represented by p_d and T_d, the distance and time for driving, represented by d_t and t_d, and the destination and corresponding parking time, represented by p_e and t_p. The trip vector is represented by Eqns (17–19).

$$\begin{aligned}&\left(p_{d,1},\ p_e,\ T_{d,1},\ t_d,\ t_p, d_t\right)\\&= \left(p_{d,1}; p_{e,1}, p_{e,2}\cdots p_{e,m}; T_{d,1}; t_{d,1}, t_{d,2}\cdots\right.\\&\left. t_{d,m}; t_{p,1}, t_{p,2}\cdots t_{p,m}; d_{t,1}, d_{t,2}\cdots d_{t,m}\right)\end{aligned} \tag{17}$$

$$T_{d,m+1} = T_{d,m} + t_d + t_p,\ m = 1,\ 2,\ 3, \ldots \tag{18}$$

$$p_{d,m+1} = p_{e,m},\ m = 1,\ 2,\ 3, \ldots \tag{19}$$

where m represents the index of trips.

A trip chain is formulated for each EV agent, which starts from leaving home at time $T_{d,1}$. The parameters of the following trips are dependent on the previous trips. The ABTCM shows very good performances of modeling real charging demand, which has been validated in the authors' previous work [43]. The energy consumption of an EV trip is assumed to be proportionate to its driving distance. The energy discharge of EV battery after a trip is measured by State of Charge (SOC), which is calculated by Eqn (20).

$$\mathrm{SOC} = \mathrm{SOC}_0 - \mathrm{d}_{t,m} * \mathrm{E}/\mathrm{C} \tag{20}$$

where SOC_0 is the original SOC before the trip; E is the electricity consumption per kilometer; and C is the capacity of EV battery.

In this study, two charging strategies, uncontrolled charging (UC) strategy and off-peak charging (OPC) strategy, are employed to simulate EV charging behaviors, and the detailed algorithm can be found in Ref. [43].

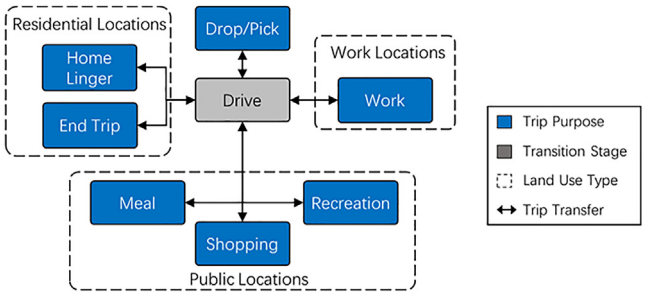

Fig. 2. Travel pattern of EVs in the agent-based trip chain model (ABTCM).

The accessibility to different types of EVSE is considered as an impact factor on EV charging behaviors. Based on the statistics in Refs. [44], EVSE is categorized into three types according to the range of power output, as shown in Table 1.

The simulation is implemented with a 1-min resolution to obtain the daily average charging demand as indicated by Eqn (21).

$$Da_{lu} = \left\{Da_{lu,1},\ Da_{lu,2}\cdots, Da_{lu,t}\right\},\ lu \in \{R, W, P\} \tag{21}$$

where Da represents the hourly average charging demand; the subscript lu denotes land use types; and R, W, P represent the residential, working and public land use type, respectively.

2.3. Cell-based geographic partition for charging demand localization

The charging demand obtained from the ABTCM simulation is localized to the studied area according to the types of land uses. As shown in Fig. 3, six types of areas including: Residential Villa Area (RVA), Residential Apartment Area (RAA), Commercial Area (CA), Working Area (WA), Mixed-use Area (MA) and Natural Area (NA), are identified by GIS. The residential charging demand obtained from the ABTCM is localized to RVAs and RAAs, while, only the charging demands originated at RAAs can be satisfied by intra-city PCSs, because residential villas are usually equipped with private EV chargers. The working charging demand is localized to WAs, and the public charging demand is localized to CAs and MAs.

In this study, the parking lots are identified as potential locations for intra-city PCSs, owing to their accessibility and convenience. Each PCS is assumed to contain enough parking places.

As shown in Fig. 3, the area is partitioned into a number of equally sized square cells. Each cell contains a certain amount of charging demand, which is also called a demand node. The charging demand is localized based on the real distribution of traffic flow, which is measured by the traffic measurement points (TMPs) in the studied area. The traffic flow in each cell (f_j) is the average value of all TMPs in it (Eqn (22)). If there is no TMP in one cell, the traffic flow is assumed to be the average of its surrounding cells. The spatial distributions of traffic flows are determined by land use type and the function of areas, as given in Eqn (23). As shown in Eqn (24), the total charging demand, which is obtained from ABTCM (Eqn (21)) is localized to the corresponding areas based on the function of traffic flows.

The original charging demand in each cell is firstly satisfied by existing PCSs (Eqn (25)) and the remaining charging demand is the potential demand for newly-built PCSs. As shown in Fig. 3, the service ability, i.e., total installed capacity, of existing PCSs is distributed to each cell in proportion to the inversion of the distance between the PCS and the cell (Eqns (26) and (27)).

$$f_j = \frac{1}{K_j} * \sum_{k_j=1}^{K_j} f_{k_j} \tag{22}$$

Table 1
EVSE output power and deployment at different land use types.

EVSE	Output power	Residential	Work	Public
Level 1	Up to 3.7 kW	✓		
Level 2	Up to 22 kW		✓	✓
Level 3	Up to 240 kW			✓

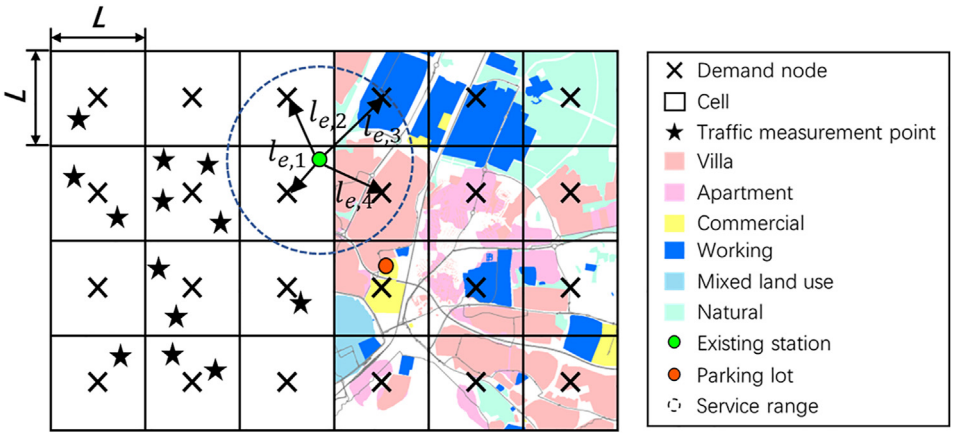

Fig. 3. An illustrative city map division and GIS identification.

$$f_{lu,j} = f_j \cdot \frac{A_{lu,j}}{A_{RAA,j} + A_{RVA,j} + A_{WA,j} + A_{CA,j} + A_{MA,j}}, \quad lu \in \{RVA, RAA, WA, CA, MA\} \tag{23}$$

$$Dc_j = Da_R \cdot \frac{f_{RAAj}}{\sum_{j=1}^{J}\left(f_{RAAj} + f_{RVAj}\right)} + D_W \cdot \frac{f_{WAj}}{\sum_{j=1}^{J} f_{WAj}} + D_P \cdot \frac{f_{CAj} + f_{MAj}}{\sum_{j=1}^{J}\left(f_{CAj} + f_{MAj}\right)} \tag{24}$$

$$Dl_{j,t} = max\left(0, Dc_{j,t} - \sum_{z=1}^{Z} De_{z,j}\right) \tag{25}$$

$$De_{z,j} = \frac{re_{z,j} * 1/le_{z,j}}{\sum_{j=1}^{J}(re_{z,j} * 1/le_{z,j})} \cdot P_z \tag{26}$$

$$re_{z,j} = \begin{cases} 1 & le_{z,j} \le L \\ 0 & le_{z,j} > L \end{cases} \tag{27}$$

where f represents the amount of traffic flow; k and K are the index and the total number of TMPs in the cell, respectively; A represents the area covered by a type of land use; and Dc_j is a 24-dimensional vector containing hourly charging demand at the node of cell j ($Dc_{j,t}$); the subscript z denotes the index of existing PCSs; De represents the charging demand on a demand node covered by an existing PCS; re is a binary variable denoting the coverage ability of an existing PCS; le represents the Euclidean distance between a demand node and an existing PCS; and P represents the total output power of an existing PCS.

3. Case study

Västerås, Sweden has an overall area of 67 km^2. There were 44,192 private vehicles including 324 plug-in EVs in 2016. In the present study, the penetration rate of EV is assumed to be 5%, which implies a total of 2200 EVs.

Sweden had achieved almost carbon-free electricity supply by 2017, and set an ambitious objective to achieve 100% renewable electricity generation by 2040 [45]. The electricity supply by source in Sweden is depicted in Fig. 4.

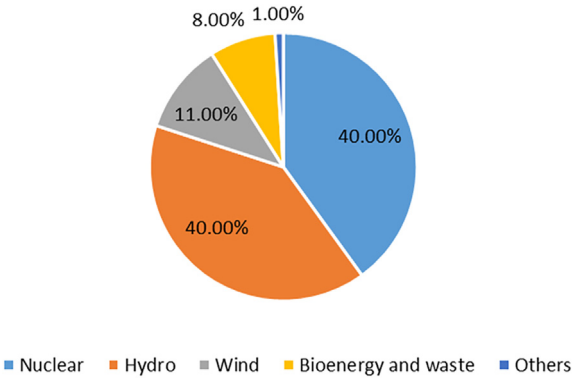

Fig. 4. The electricity supply by source in 2017 in Sweden. Data source: IEA [45].

The transport sector, consuming a large amount of oil, accounts for half of Swedish energy-related carbon emissions. Sweden aims to reduce 70% of greenhouse gas emissions of the transport sector from 2010 to 2030. Therefore, electrification of transport has been vigorously promoted, and public charging infrastructure has been greatly developed to strengthen the confidence of consumers. In 2017, Sweden had b the highest proportion of EV sales in the world, i.e., 6.3% in new car sales.

Fig. 5 shows the distribution of different types of land uses, which is derived from OpenStreetMap and Google Earth. As shown in Fig.5(a), 8 PCSs with 40 chargers have already been installed in the city [46]. A total of 532 parking lots in this area are identified as potential locations for newly built intra-city PCSs. The map of the parking lots shown in Fig. 5(b), is obtained from OpenStreetMap [47]. As shown in Fig. 5(c), the traffic flow is monitored at 245 TMPs, and the data can be obtained from the traffic administration of Västerås [48]. The whole city is divided into 268 cells with the side length of 500 m as illustrated in Fig. 5(d).

The travel patterns are determined based the American National Household Travel Survey 2017 and some key parameters, i.e. departure time, travel distance and travel time, are calibrated by Swedish National Travel Survey (2015–2016) [49,50]. The charging patterns are extracted from an EV project [38].

The output power of EVSE and the cost for charging are taken from the existing PCSs in Västerås, Sweden [46], as shown in Table 2. In this paper, Level 2 and Level 3 EVSE are referred to as slow and fast chargers, respectively. According to the types of EVSE, the PCSs are referred to as Slow PCSs (SPCSs) and Fast PCSs (FPCSs), respectively. It is assumed that each PCS has at least 1 charger and at most 20 chargers. It is also assumed that FPCS will be constructed

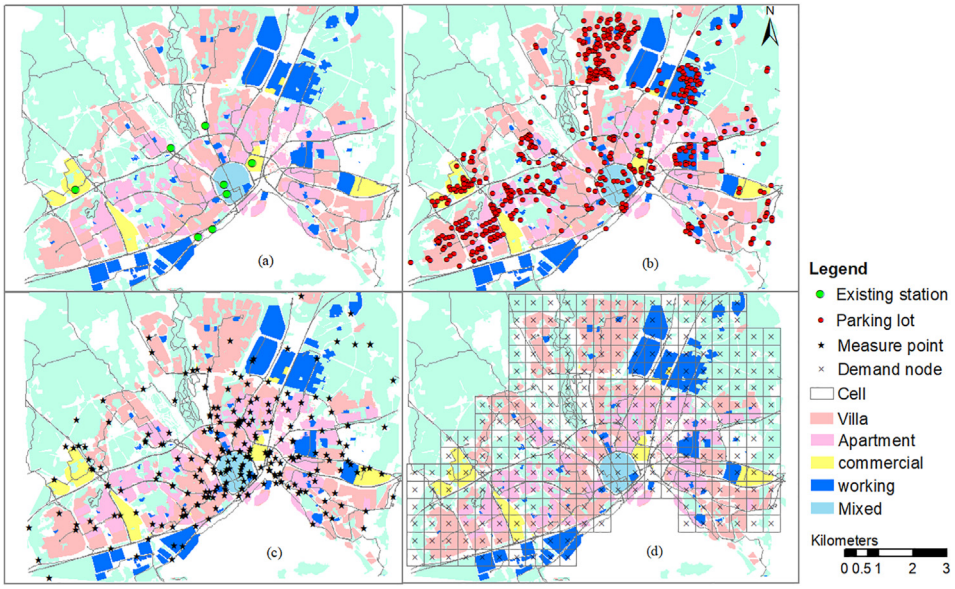

Fig. 5. GIS information on transportation and E.V. charging in Västerås, Sweden.

Table 2
The parameters of EVSE.[a]

EVSE	Output power	Charge Price	Investment costs	Lifetime
Level 2	12.8 kW	1 SEK/min	$7350 per unit	10 years
Level 3	48 kW	3 SEK/min	$33650 per unit	10 years

[a] 1 $ = 8.66 SEK; Electricity price: 0.5 SEK/kWh.

To evaluate the impacts of charging strategies, service range and economic parameters on the profits of PCSs, four scenarios are generated, and the first scenario is a benchmarking scenario. Scenario 2 simulates the EV charging demand under the OPC strategy where EV owners are motivated to change their charging patterns to improve the grid reliability. Scenario 3 focuses on the impacts of

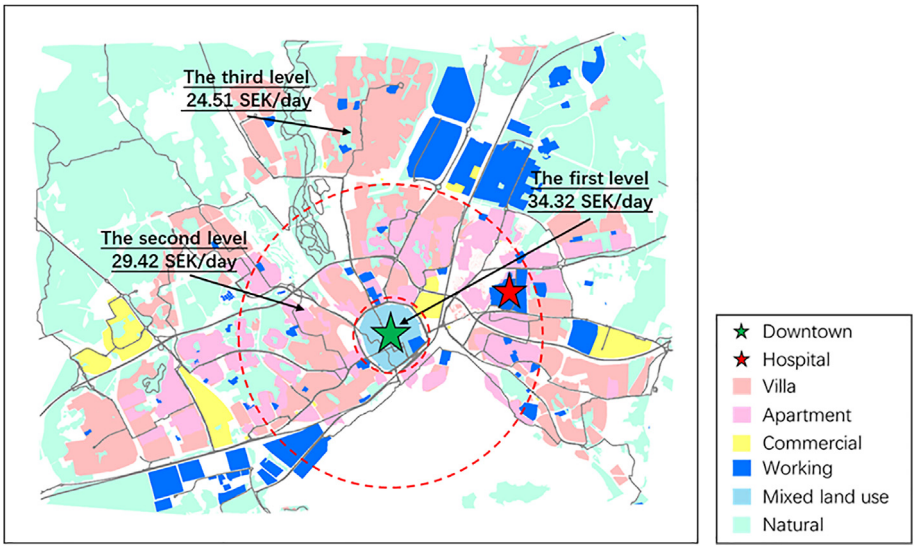

Fig. 6. Classification of studied area based on land rental costs.

only in CAs and SPCSs in WAs and RAAs. In addition, the parameters of Nissan Leaf EV are adopted to represent typical EV parameters.

As shown in Fig. 6, the city is divided into three zones, corresponding to different land rental costs. Downtown in the inner ring (green star) has the highest land cost, and the hospital (red star) is the demarcation point of the second ring and the third ring. The information on EVSE is summarized in Table 2. The investment costs are derived from Refs. [42,51], which are commonly used by other literature.

Table 3
Scenarios on intra-city PCS planning.

Scenario	Charging strategy	Service range	Charging price
1	UC	500 m	Fixed
2	OPC	500 m	Fixed
3	UC	1000 m	Fixed
4	UC	500 m	Sensitivity analysis

coverage ability of PCSs, where a larger service range, 1000 m, is considered. In Scenario 4, a sensitivity analysis on charging price is conducted. The details of the scenarios are tabulated in Table 3. In each scenario, three optimizations are conducted with the number of newly-built PCSs being no more than 5, 10 and 15. In addition, the number of EVs is assumed to remain the same.

4. Results and discussion

4.1. Benchmarking scenario

The ABTCM is used to simulate the charging demand of 2200 EVs. To capture the comprehensive randomness of EV behaviors, the simulation was carried out for 77 days with a time step of 1 min. The simulation of the first seven days is removed to ensure that the battery SOC of the EV fleet have arrived in random states, and the following results start from the 8th day of simulation.

Fig. 7 shows the typical one-day charging profiles at different land use types. The charging demand in a specific hour of day is averaged over the values of charging demand in the same hour of the 70 simulation days. The derived typical one-day charging profiles reflect the different travel and charging patterns on weekday and weekend. It is found that a large portion of daily charging demand is met at residential land use types, and 65% of the portion is satisfied in RVAs, which is not included in public charging demand. The peak of public charging demand appears at around 9 o'clock in the morning, which is mainly contributed by the charging demand in WAs and CAs.

To understand the impacts of the number of newly-built PCSs, it was assumed that 5, 10 and 15 PCSs would be built, and the optimized number of chargers, costs, and profits for all PCSs are listed in Table 4. The overall economic performances of the newly built PCSs are very good, mainly due to the high charging price in Västerås, which is 7.5–9.4 times of the electricity price. The charging demand covered by an average PCS increases with the total number of PCSs. The increase in covered charging demand simultaneously raises the profit and reduces the payback time. In contrast, the return on investments (ROI) decreases with the increase in the number of PCS, i.e., the ROI is 409.7%, 396.3%, and 375.3% for 5, 10 and 15 newly built PCSs, respectively, which indicates that the ROI is affected by the utilization rate of chargers.

Table 4
Results of PCS planning in Scenario 1.

Number of newly-built PCS	5	10	15
FPCS/SPCS number	1/4	2/8	3/12
Fast/Slow Charger number	1/18	2/28	3/35
Covered demand (kWh/day)	2663.4	3903.8	4763.8
Covered public demand fraction (%)	31.1	45.6	55.7
Profit (SEK/day)	9641.3	13857.6	16816.1
Cost (SEK/day)	2353.4	3587.5	4480.5
ROI (%)	409.7	396.3	375.3
Payback time (days)	143	163	176

The locations of the PCSs are illustrated in Fig. 8. Since most existing PCSs are in the city center, the newly-built PCSs are mainly located in the surrounding area. However, in general, the PCSs closer to the central tend to have a high level of profits due to a high level of charging demand.

4.2. The impacts of charging pattern

With the development of smart charging technologies, it is foreseen that off-peak charging will be greatly promoted, where EV owners are motivated to charge at home and reduce their reliance on PCSs [52]. As shown in Fig. 9, almost all the charging demand is shifted to evening time, and resultantly the charging demand in CAs and WAs is shifted to residential areas.

Although the total amount of charging demand remains unchanged, the public charging demand decreases rapidly. This causes a high peak of charging demand in the residential areas, of which the magnitude is twice larger than the peak in Scenario 1.

The detailed results are reported in Table 5. The change in charging patterns leads to significant decrease in profits (compared to Table 4). Yet, covered demand remains increasing, and the payback time decreases with the number of PCSs. However, the type, location and number of chargers of the newly-built PCSs are different from those in the benchmarking scenario. Compared to the benchmarking scenario, all the newly-built PCSs are SPCSs in residential areas and the total public charging demand in Scenario 2 is reduced by about 40%, resulting in fewer number of chargers on

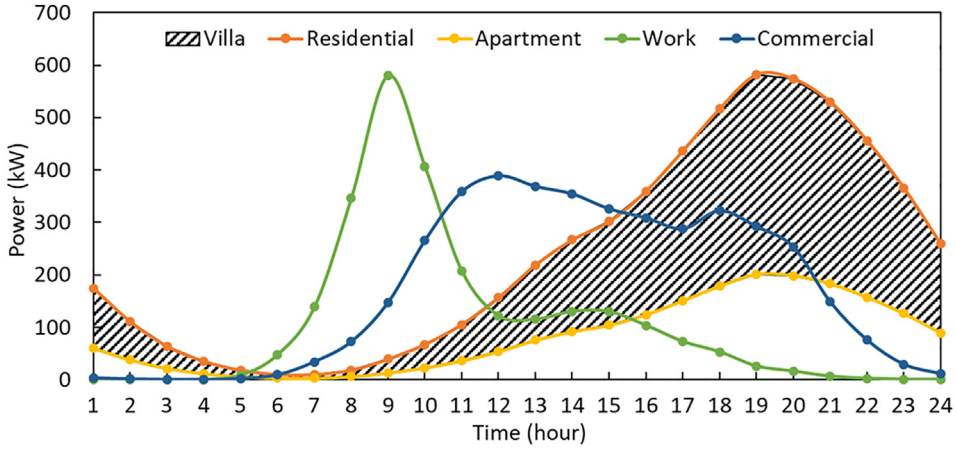

Fig. 7. Typical EV charging demand profiles at different land use types under the UC strategy.

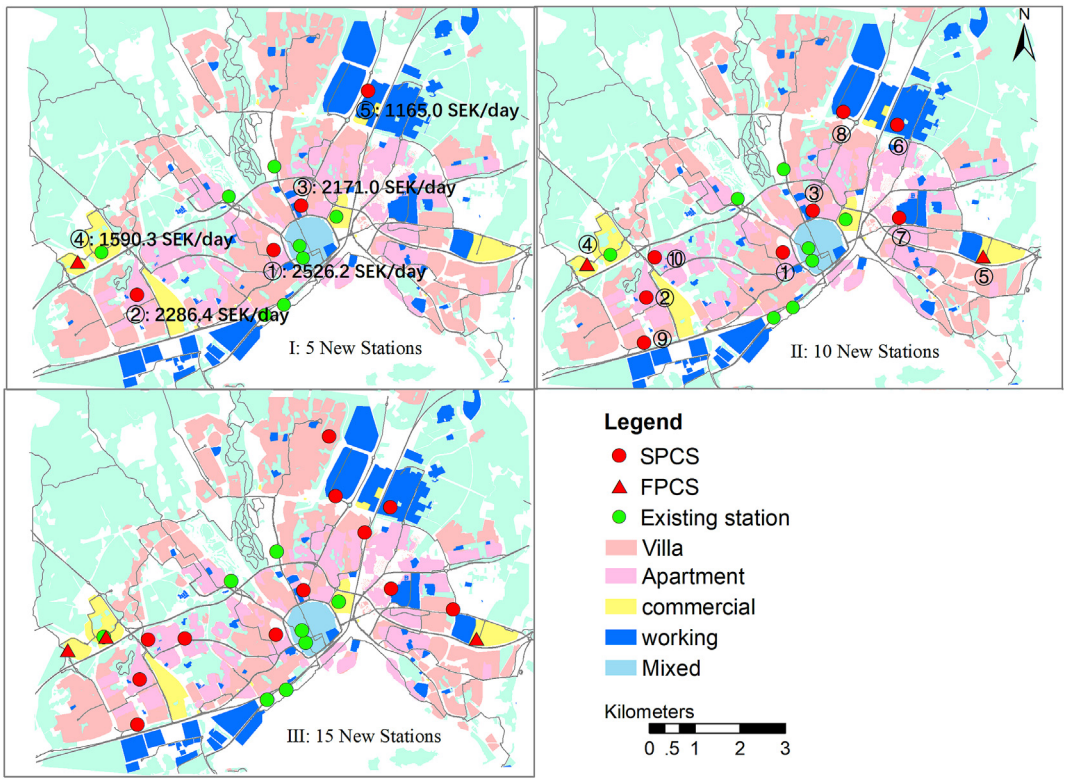

Fig. 8. Locations and daily profits of the newly-built PCSs in Scenario 1.

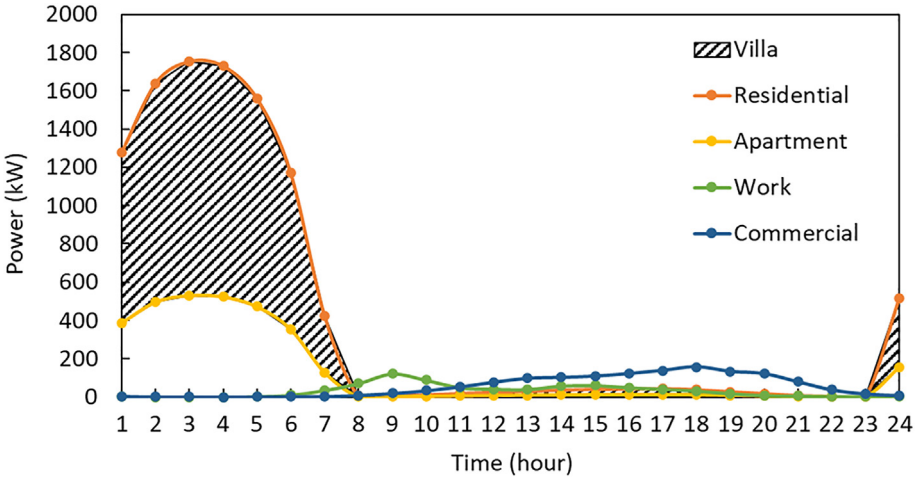

Fig. 9. Typical EV charging demand profiles at different land use types under OPC strategy.

Table 5
Results of PCS planning in Scenario 2.

Number of newly-built PCS	5	10	15
FPCS/SPCS number	0/5	0/10	0/15
Fast/Slow Charger number	0/14	0/27	0/34
Covered demand (kWh/day)	1356.1	2334.8	2934.4
Covered public demand fraction (%)	26.0	44.8	56.4
Profit (SEK/day)	4978.5	8443.6	10406.1
Cost (SEK/day)	1378.2	2501.0	3217.3
ROI (%)	361.2	337.6	323.4
Payback time (days)	171	193	216

average at every PCS.

4.3. The impacts of the coverage ability of PCSs

Service range is an important indicator for evaluating PCS service ability. Exiting studies assumed that service range should be slightly longer than people's acceptable walking distance from parking lots to destinations, i.e., 400 m. Some studies adopted the service range of refueling station. Regarding SPCS, EV owners usually park vehicles for a long period of time, and the service range

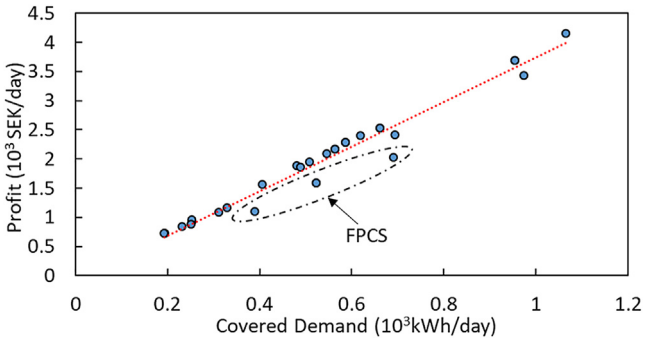

Fig. 10. Correlation between covered demand and daily profit of the new PCSs.

should be close to the acceptable walking distance to avoid impairing people's travel satisfaction. However, in anticipation of the advancement of fast charging and battery swap technology, the duration to serve a customer will become shorter and close to the service time of refueling station. Therefore, this study sets up service range of 500 m and 1000 m to investigate the impacts of cover ability.

For a certain type of PCS, a larger service range usually means a larger amount of covered charging demand, and thus means larger charging revenues. The relation between coverage ability and daily profits is illustrated in Fig. 10, based on the results for 5 and 10 PCSs in Scenario 1 and 3. Fig. 10 reflects that profit is linearly correlated to charging demand, which is under the limit that a PCS can serve. The profitability of FPCS is slightly lower than that of SPCS, because FPCS has higher investment. The comparison between FPCS and SPCS will be elaborated in Section 4.4.1. In addition to service range, larger penetration rates also mean larger amount of charging demand for each PCS. Given the lessons learned here, the profit of PCS will increase proportionally with the increase in EV penetration rate, while the return-on-investment (ROI) of PCS is similarly constant. Since the number of chargers has not reached the capacity limit, the number of chargers will increase with the increase in charging demands, while the locations of PCSs remain the same. If the penetration of EVs keeps increasing and reaches the capacity of potential locations, new PCSs will be built and the locations with high profitability have priority over others (Fig. 8).

The numerical results of Scenario 3 are presented in Table 6. Compared to the benchmarking scenario, the covered charging demand in Scenario 3 is 58.8% larger with 5 newly-built PCSs, 46.5% larger with 10 newly-built PCSs and 31.4% larger with 15 newly-built PCSs. Correspondingly, the number of chargers increases by 57.9%–89.5%, and the profits increase by 38.7%–57.5%. The covered demand of a charger on average is less than that in Scenario 1, which indicates a decrease in charger utilization as well as ROI.

Fig. 11 depicts the cover ability of existing and newly-built PCSs in Scenario 1 and 3. The public charging demand covered by existing PCSs increases from 691.9 kWh in Scenario 1 to 1987.3 kWh in Scenario 3, accounting for about 23% of the total public charging demand. As shown in Fig. 11(d), the existing and newly-built PCSs with a service range of 10000 m can meet 95% of the total public charging demand. In addition, disproportionately huge investment is needed to meet the remaining 5% of the peak public charging demand. This will be discussed in detail in Section 4.4.2.

Table 6
Results of PCS planning in Scenario 3.

Number of newly-built PCS	5	10	15
FPCS/SPCS number	1/4	0/10	0/15
Fast/Slow Charger number	2/34	0/50	0/60
Covered demand (kWh/day)	4229.4	5718.6	6259.7
Covered public demand fraction (%)	49.4	66.8	73.1
Profit (SEK/day)	15184.4	21538.6	23322.5
Cost (SEK/day)	3994.1	5267.5	6019.7
ROI (%)	380.2	408.9	387.4
Payback time (days)	172	142	157

4.4. The impacts of charging price

The high charging price in Västerås is expected to decline in the future and this would encourage people to charge at PCSs. In this section, the impacts of charging price are evaluated by a sensitivity analysis.4.4.1 The impacts on the competition between FPCS and SPCS.

The cost for a FPCS is generally higher than that for a SPCS (Table 2). One the one hand, the investment costs and O&M cost of a FPCS are higher than that of a SPCS. On the other, the fee charged per kWh at a FPCS is 80% of that at a SPCS. Therefore, SPCSs have higher profitability than FPCSs for serving the same amount of charging demand. This explains why the number of SPCS is usually much more than the number of FPCS.

To investigate the impacts of charging price on the competition between FPCS and SPCS, the charging price of FPCS is fixed, while the charging price of SPCS decreased by 0%–50%, with a step of 5%. The variation in the number of FPCS is shown in Fig. 12. The reduction in charging price of SPCS leads to a declining profitability as well as competitiveness, while the number of FPCSs increases. When the reduction in charging price of SPCS is smaller than 25%, the number of FPCS is fewer than the number of SPCS; when the charging price of SPCS reduces by 25%–30%, FPCS becomes competitive with SPCS; and the number of FPCS is more than the number of SPCS when the charging price of SPCS decrease over 35%. However, maximum 8 FPCSs could be constructed in a total of 15 PCSs, due to the limit of the total commercial land use area.

The geographical distribution of the 5 new PCSs with a 15% and a 45% reduction in SPCS charging price is shown in Fig. 13. Compared to the benchmarking scenario, SPCSs are replaced by FPCS, while the location of the PCSs remains nearly unchanged. This result reflects the fact that the PCS location mainly depends on the distribution of aggregated charging demand, and it certifies the robustness of the proposed method for optimizing PCS location.

4.4.1. The impacts on PCS payback time and sizing

To investigate the impacts of price variation on PCS payback time and sizing, the charging prices of both SPCS and FPCS decrease by 0%–80%, with a step of 10%. For SPCS, a 25% reduction in the charging price is taken as the reference for the sensitivity analysis.

The variation of ROI and payback time for 10 newly-built PCSs with different charging prices is illustrated in Fig. 14. ROI decreases and the payback time increases with the reduction in charging price. PCSs will break even when the charging price reduces by 80%, while the payback time prolonged to about ten years.

Variation of charging price also impacts on PCS sizing, which can further affect the coverage ability of PCSs. As depicted in Fig. 15, the charging capacity of PCSs decreases, and average working time increases along with the reduction of charging price. Compared to the benchmarking scenario, the peak charging power decreases by about 80% and the average daily working time of chargers increases from 8.6 h to 11.8 h, due to an 80% reduction in charging price.

To further evaluate the impacts of charging price on the coverage ability of PCS, a random SPCS is taken as an example. As shown in Fig.16Fig.16, the peak demand can be satisfied by 3 chargers. When the charging price is reduced by 60%, indicated by the grey dashed curve, the optimization results show that only one

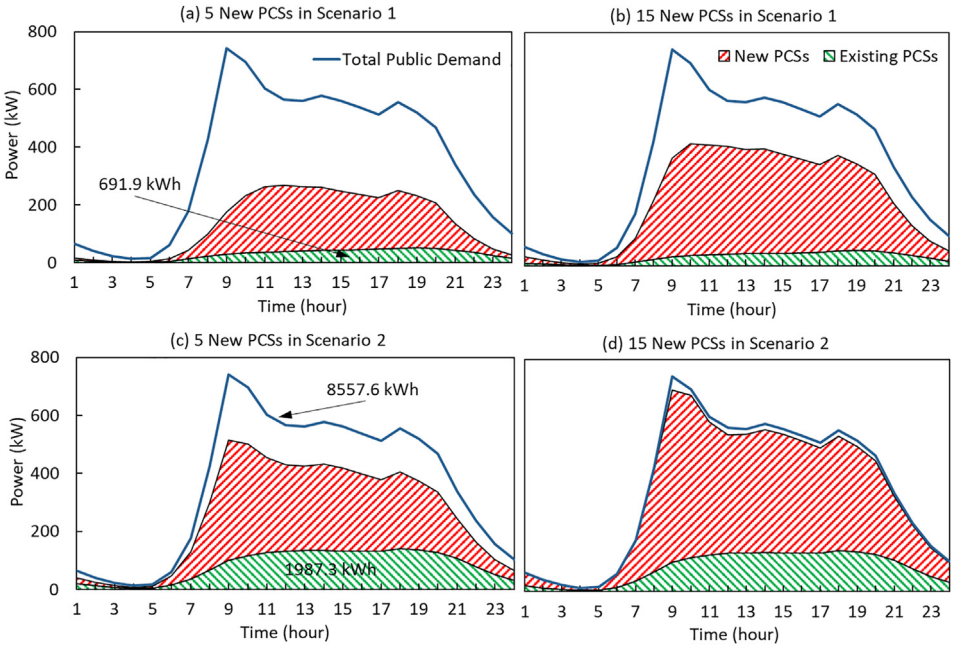

Fig. 11. Public charging demand covered by existing and new PCSs in Scenario 1 and 3.

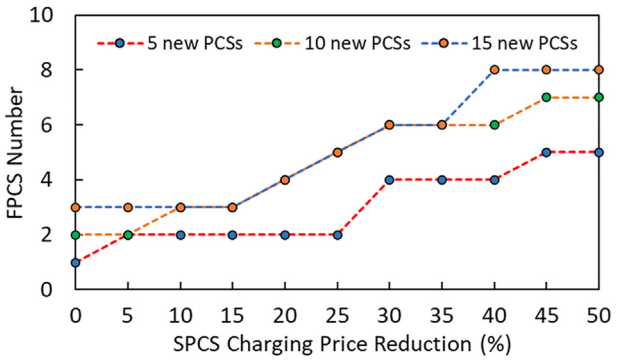

Fig. 12. The impacts of SPCS charging price reduction on the planning of FPCSs.

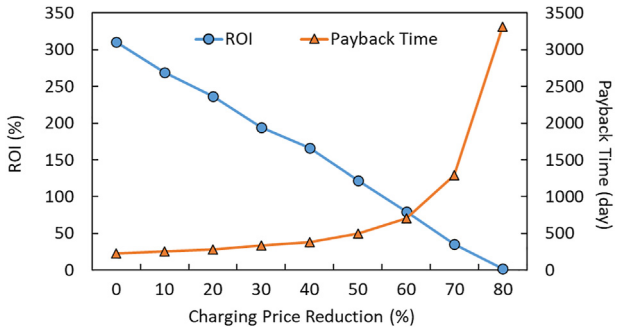

Fig. 14. Variation of ROI and payback time with different charging prices.

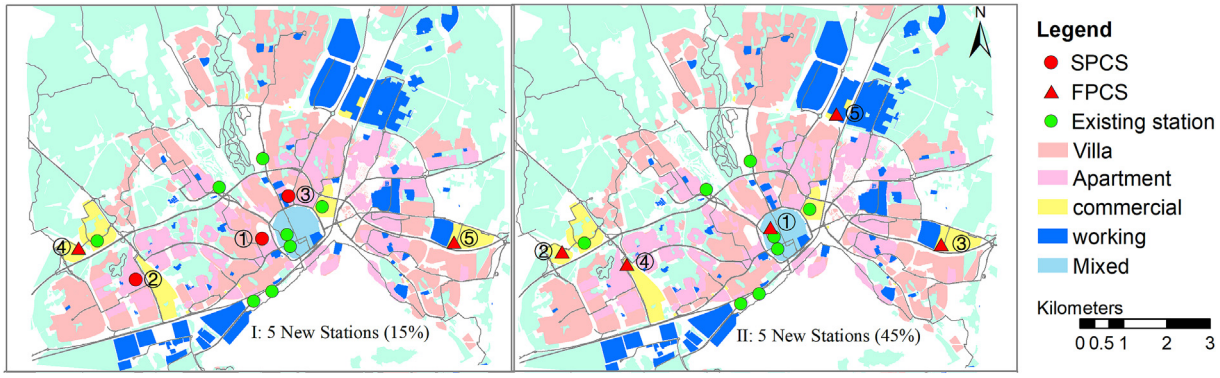

Fig. 13. Overview of the siting results with a 15% and a 45% reduction in SPCS charging price of.

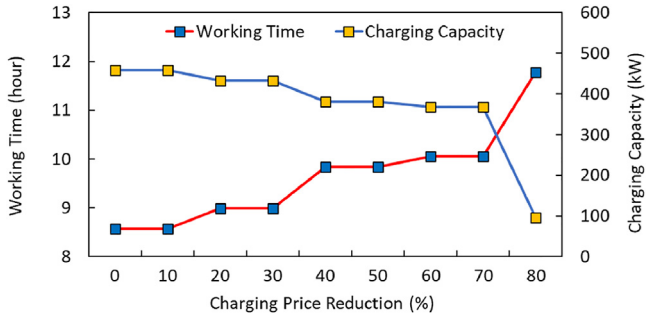

Fig. 15. Variation of average working time and covered charging power with different charging prices.

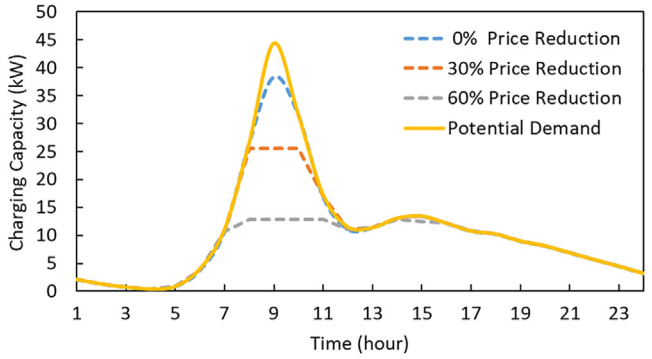

Fig. 16. The ability of a PCS to cover peak demand with different charging prices.

charger will be installed, and only the base demand will be met. The results with a high time resolution further prove the advantage of the proposed model in modeling the temporal heterogeneity of stochastic charging demand.

5. Conclusion

To optimize the location and size of Public Charging Stations (PCSs) and in order to maximize their profits, this paper proposes a framework, which combines an ABTCM, a cell-based geographic partition method and a GIS-based MILP optimization model. Such a framework provides a robust and adaptable approach to distinguish public charging demand from private charging demand and provides a real representation of the spatial and temporal distribution of public charging demand. The method has a good replicability. It can be applied to any city if the travel survey data, traffic flow measurement, and distribution of parking lot locations are available.

In this work, the proposed framework is verified by adopting it for a case study. The impacts of charging pattern, coverage ability of PCS and charging price on the planning of PCSs are specifically investigated. With the current charging price, the more charging demand a PCS serves, the higher profits it attains. Public charging demand can decrease by as much as 40% due to the variation of charging pattern, and the profits of a PCS would decrease significantly under the off-peak charging strategy. Due to the same reason, improving the coverage ability of a PCS can improve its profitability, and the location of PCSs gives priority to the areas with high charging demand. In addition, a decrease in charging price impairs the profitability of PCSs, and thus leads to smaller PCS sizes. By comparison, SPCS has competitiveness advantage over FPCS with the current charging price, while FPCS becomes competitive with SPCS when the charging price of SPCS reduces by 25%–30%.

This paper provides policy makers and PCS investors an effective tool for planning intra-city PCS investments and highlights the importance of charging prices for motivating EV penetration. This work focuses on the planning of PCS in reference to profitability and the capacity limit of the local low-voltage grid was not considered, due to lack of data. Future studies will consider the variation of charging speed and the impacts on low-voltage distribution network based on real-time distributed control algorithm for EV charging and vehicle to grid (V2G). In addition, in the current study, the demand simulation and PCS planning are relatively independent to avoid changing the existing travel and charging pattern of drivers. The impacts of newly-built PCSs on the travel and charging behaviors of EV owners can be evaluated in a more interactive way in future studies.

Credit author statement

Haiyang Lin: Conceptualization, Methodology, Software, Formal analysis, Writing – original draft, Writing – review & editing. **Caiyun Bian:** Conceptualization, Methodology, Software, Investigation, Resources, Writing – original draft. **Yu Wang:** Formal analysis, Writing – original draft, Writing – review & editing. **Hailong Li:** Conceptualization, Funding acquisition, Writing – review & editing, Supervision, Project administration. **Qie Sun:** Writing – review & editing, Funding acquisition, Supervision. **Fredrik Wallin:** Conceptualization, Investigation, Funding acquisition, Project administration. These authors contributed equally: **H.L.**, **C.B.** and **Y.W.**

Declaration of competing interest

The authors declare that they have no known competing financial interests or personal relationships that could have appeared to influence the work reported in this paper.

Acknowledgements

The authors would like to thank the support from Program for Outstanding PhD Candidate of Shandong University, China Scholarship Council, Gustav Dahl Scholarship of Mälardalen University, National Natural Science Foundation of China (Project U1864202), Shandong University Seed Fund Program for International Research Cooperation, and KK-stiftelsen (Synergi 19-FLEXERGY, 20200073).

References

[1] Zhang L, et al. Hybrid electrochemical energy storage systems: an overview for smart grid and electrified vehicle applications. Renew Sustain Energy Rev 2021;139:110581.
[2] van der Steen M, et al. EV policy compared: an international comparison of governments' policy strategy towards E-mobility. In: Kotter R, editor. *E-Mobility in Europe: Trends and good practice*, W. Leal filho and. Cham: Springer International Publishing; 2015. p. 27–53.
[3] Patrick H, et al. Expanding electric-vehicle adoption despite early growing pains. McKinsey Center for Future Mobility; 2019.
[5] Guo F, Yang J, Lu J. The battery charging station location problem: impact of users' range anxiety and distance convenience. Transport Res E Logist Transport Rev 2018;114:1–18.
[6] Wiederer A, Philip R. Policy options for electric vehicle charging infrastructure in C40 cities. 2010.
[7] IEA. Global EV Outlook 2020. Paris: IEA; 2020. https://www.iea.org/reports/global-ev-outlook-2020.
[8] Zhang Q, et al. Factors influencing the economics of public charging infrastructures for EV – a review. Renew Sustain Energy Rev 2018;94:500–9.
[9] Cavadas J, Homem de Almeida Correia G, Gouveia J. A MIP model for locating slow-charging stations for electric vehicles in urban areas accounting for driver tours. Transport Res E Logist Transport Rev 2015;75:188–201.
[10] Sun Z, et al. Locating charging stations for electric vehicles. Transport Policy; 2018.
[11] Xi X, Sioshansi R, Marano V. Simulation–optimization model for location of a

public electric vehicle charging infrastructure. Transport Res Transport Environ 2013;22:60–9.
[12] Wang Y, et al. Siting and sizing of fast charging stations in highway network with budget constraint. Appl Energy 2018;228:1255–71.
[13] Zhu Z-H, et al. Charging station location problem of plug-in electric vehicles. J Transport Geogr 2016;52:11–22.
[14] Arkin EM, et al. Locating battery charging stations to facilitate almost shortest paths. Discrete Appl Math 2019;254:10–6.
[15] Gagarin A, Corcoran P. Multiple domination models for placement of electric vehicle charging stations in road networks. Comput Oper Res 2018;96:69–79.
[16] Sadeghi-Barzani P, Rajabi-Ghahnavieh A, Kazemi-Karegar H. Optimal fast charging station placing and sizing. Appl Energy 2014;125:289–99.
[17] Awasthi A, et al. Optimal planning of electric vehicle charging station at the distribution system using hybrid optimization algorithm. Energy 2017;133:70–8.
[18] Zhou J, et al. A geographical information system based multi-criteria decision-making approach for location analysis and evaluation of urban photovoltaic charging station: a case study in Beijing. Energy Convers Manag 2020;205:112340.
[19] Fathabadi H. Novel wind powered electric vehicle charging station with vehicle-to-grid (V2G) connection capability. Energy Convers Manag 2017;136:229–39.
[20] Schroeder A, Traber T. The economics of fast charging infrastructure for electric vehicles. Energy Pol 2012;43:136–44.
[21] Yıldız B, Olcaytu E, Şen A. The urban recharging infrastructure design problem with stochastic demands and capacitated charging stations. Transp Res Part B Methodol 2019;119:22–44.
[22] He Y, Kockelman KM, Perrine KA. Optimal locations of U.S. fast charging stations for long-distance trip completion by battery electric vehicles. J Clean Prod 2019;214:452–61.
[23] Wang C, et al. Designing locations and capacities for charging stations to support intercity travel of electric vehicles: an expanded network approach. Transport Res C Emerg Technol 2019;102:210–32.
[24] Csiszár C, et al. Urban public charging station locating method for electric vehicles based on land use approach. J Transport Geogr 2019;74:173–80.
[25] Hodgson MJ. A flow-capturing location-allocation model. Geogr Anal 1990;22(3):270–9.
[26] He J, et al. An optimal charging station location model with the consideration of electric vehicle's driving range. Transport Res C Emerg Technol 2018;86:641–54.
[27] Zhang J, et al. A modified MOEA/D approach to the solution of multi-objective optimal power flow problem. Appl Soft Comput 2016;47:494–514.
[28] Yang W. A user-choice model for locating congested fast charging stations. Transport Res E Logist Transport Rev 2018;110:189–213.
[29] Li S, Huang Y, Mason SJ. A multi-period optimization model for the deployment of public electric vehicle charging stations on network. Transport Res C Emerg Technol 2016;65:128–43.
[30] Wu F, Sioshansi R. A stochastic flow-capturing model to optimize the location of fast-charging stations with uncertain electric vehicle flows. Transport Res Transport Environ 2017;53:354–76.
[31] Chung SH, Kwon C. Multi-period planning for electric car charging station locations: a case of Korean Expressways. Eur J Oper Res 2015;242(2):677–87.
[32] Toregas C, et al. The location of emergency service facilities. Oper Res 1971;19(6):1363–73.
[33] Daina N, Sivakumar A, Polak JW. Modelling electric vehicles use: a survey on the methods. Renew Sustain Energy Rev 2017;68(Part 1):447–60.
[34] Vazifeh MM, et al. Optimizing the deployment of electric vehicle charging stations using pervasive mobility data. Transport Res Pol Pract 2019;121:75–91.
[35] Bai X, Chin K-S, Zhou Z. A bi-objective model for location planning of electric vehicle charging stations with GPS trajectory data. Comput Ind Eng 2019;128:591–604.
[36] Frade I, et al. Optimal location of charging stations for electric vehicles in a neighborhood in Lisbon, Portugal. Transport Res Rec 2011;2252(1):91–8.
[37] Alhazmi YA, Salama MMA. Economical staging plan for implementing electric vehicle charging stations. Sustain Energy Grids Network 2017;10:12–25.
[38] Smart J, Schey S. Battery electric vehicle driving and charging behavior observed early in the EV project. SAE Int 20;1(1):27–33.
[39] Erbaş M, et al. Optimal siting of electric vehicle charging stations: a GIS-based fuzzy Multi-Criteria Decision Analysis. Energy 2018;163:1017–31.
[40] Ren X, et al. Location of electric vehicle charging stations: a perspective using the grey decision-making model. Energy 2019;173:548–53.
[41] Luo L, et al. Optimal planning of electric vehicle charging stations comprising multi-types of charging facilities. Appl Energy 2018;226:1087–99.
[42] Cregger J. Charging infrastructure required to support US electric vehicle deployment: a cost estimate through 2025. In: 2015 IEEE vehicle power and propulsion conference (VPPC). IEEE; 2015.
[43] Lin H, et al. Characteristics of electric vehicle charging demand at multiple types of location - application of an agent-based trip chain model. Energy 2019;188:116122.
[44] Flores RJ, Shaffer BP, Brouwer J. Electricity costs for an electric vehicle fueling station with Level 3 charging. Appl Energy 2016;169:813–30.
[45] Agency IE. Sweden 2019 review. International Energy Agency; 2019.
[46] Laddstationer i Laddregion Mälardalen. 2018. Available from: https://www.malarenergi.se/el/ladda-elbil/.
[47] Hawkes AD, Leach MA. Modelling high level system design and unit commitment for a microgrid. Appl Energy 2009;86(7):1253–65.
[48] Välkommen till Vägtrafikflödeskartan. 2018. Available from: http://vtf.trafikverket.se/SeTrafikinformation.
[49] Ai X-g, et al. Forecasting method for electric vehicle daily charging curve. Proc CSU-EPSA 2013;25(6):25–30.
[50] Ürge-Vorsatz D, Novikova A. Potentials and costs of carbon dioxide mitigation in the world's buildings. Energy Pol 2008;36(2):642–61.
[51] Smith M, Castellano J. Costs associated with non-residential electric vehicle supply equipment: factors to consider in the implementation of electric vehicle charging stations. 2015.
[52] Guo C, Chan CC. Analysis method and utilization mechanism of the overall value of EV charging. Energy Convers Manag 2015;89:420–6.